

Examination of the Critical Velocity for Deposition of Particles in Cold Spraying

Chang-Jiu Li, Wen-Ya Li, and Hanlin Liao

(Submitted August 9, 2005; in revised form January 3, 2006)

The critical velocity of copper (Cu) particles for deposition in cold spraying was estimated both experimentally and theoretically. An experimental method is proposed to measure the critical velocity based on the theoretical relationship between deposition efficiency and critical velocity at different spray angles. A numerical simulation of particle impact deformation is used to estimate the critical velocity. The theoretical estimation is based on the critical velocity corresponding to the particle velocity at which impact begins to cause adiabatic shear instability. The experimental deposition was conducted using Cu particles of different particle sizes, velocities, oxygen contents, and temperatures. The dependency of the critical velocity on particle temperature was examined. Results show that the critical velocity can be reasonably measured by the proposed test method, which detects the change of critical velocity with particle temperature and oxygen content. The Cu particles of oxygen content 0.01 wt.% yielded a critical velocity of about 327 m/s. Experiments show that the oxygen content of powder significantly influences the critical velocity. Variations in oxygen content can explain the large discrepancies in critical velocity that have been reported by different investigators. Critical velocity is also found to be influenced by particle temperature as well as types of materials. High particle temperature causes a decrease in critical velocity. This effect is attributed to the thermal softening at elevated temperatures.

Keywords adiabatic shear instability, cold spraying, critical velocity, Cu powder, deposition efficiency

1. Introduction

Cold spraying is a new emerging coating technology. In this process, a coating is formed through the plastic deformation of spray particles that are in a completely solid state during impact. The temperature of spray particles prior to impact is much lower than the melting point of the spray materials. Therefore, spray materials experience little microstructure change, oxidation, or decomposition (Ref 1). Most metals and their alloys can be deposited by cold spraying (Ref 1). Even cermets (Ref 2) can be deposited, and ceramic particles (Ref 3) can be embedded into a metal substrate to form a thin-layer coating.

It has been widely accepted that particle velocity prior to impact is one of the most important parameters in cold spraying. It determines whether deposition of a particle or erosion of a substrate occurs on the impact of a spray particle. Generally, for a given material, there exists a critical velocity such that a transition from erosion of the substrate to deposition of the particle

occurs. Only those particles achieving a velocity higher than the critical one can be deposited to produce a coating. The critical velocity is associated with properties of the spray material (Ref 1, 4) and the substrate (Ref 4-6). On the other hand, the particle velocity of a material is related to the physical properties of the driving gas, its operating pressure and temperature, as well as the nozzle design of the spray gun (Ref 7-10). The characteristics of the powder, such as density, particle size (Ref 7-10), and morphology (Ref 10, 11) also influence the particle acceleration and subsequent deposition. Although different critical velocities for copper (Cu) particles have been reported as approximately 500 m/s (Ref 1), 550 to 570 m/s (Ref 5), and 640 m/s (Ref 7) by different investigators, the underlying factors influencing particle deposition are still not well understood. An examination of the literature (Ref 1, 5, 7) showed that the differences may be due to various features of Cu powders and to the different gas conditions used in the studies. Therefore, it is necessary to investigate the factors influencing the critical velocity for particle deposition in cold spraying.

Recently, a theoretical model for the prediction of deposition efficiency in cold spraying was established (Ref 12). This model can be used to estimate the critical velocity of a particle under different spray conditions. A simple description of the model is presented in section 2.

Recent studies on solid particle impact behavior have revealed that localized plastic deformation increases with particle velocity and causes adiabatic shear instability when the velocity reaches a certain critical value (Ref 13, 14). This critical velocity is comparable to the observed critical velocity for particle deposition. Consequently, it is considered that the critical velocity for particle deposition can be estimated through the numerical simulation of impact deformation behavior from particle impact.

This article presents the deposition efficiency of powder particles with particle size distribution as a function of particle size

The original version of this paper was published in the CD ROM *Thermal Spray Connects: Explore Its Surfacing Potential*, International Thermal Spray Conference, sponsored by DVS, ASM International, and IIW International Institute of Welding, Basel, Switzerland, May 2-4, 2005, DVS-Verlag GmbH, Düsseldorf, Germany.

Chang-Jiu Li and **Wen-Ya Li**, State Key Laboratory for Mechanical Behavior of Materials, School of Materials Science and Engineering, Xi'an Jiaotong University, Xi'an, Shaanxi 710049, People's Republic of China; and **Hanlin Liao**, LERMPS, Université de Technologie de Belfort-Montbéliard, Site de Sévenans, 90010 Belfort Cedex, France. Contact e-mail: licj@mail.xjtu.edu.cn.

distribution parameters, spray angle, and critical velocity. A measurement approach for the critical velocity in cold spraying is proposed. Accordingly, the critical velocity of Cu powders was measured through relative deposition efficiency. The measurement was performed for copper particles with different oxygen contents and different particle size distributions. The critical velocity was also examined by the simulation of particle impact behavior. The effect of particle temperature on its critical velocity for deposition was investigated through both numerical simulation and experimental measurement.

2. Theoretical Relationships Among Deposition Efficiency, Critical Velocity, and Spray Angle in Cold Spraying

When spray particles are fed into a gas stream, the acceleration of each particle theoretically depends on its size. Smaller particle achieves greater acceleration, while larger particles achieve less acceleration. Consequently, the accelerations of spray particles by accelerating gas yield a velocity distribution of a particle stream. Only particles with velocity higher than a critical velocity can contribute to the buildup of a coating in cold spraying. In this study, the deposition of particles will be considered through particle size distribution and its effect on particle velocity.

To derive the deposition efficiency as a function of particle size distribution and critical velocity, as a first approximation, the following assumptions are made (Ref 12).

- All particles of a normal velocity higher than the critical velocity are deposited on the substrate.
- The critical velocity for particle deposition is independent on particle size for one specific powder.
- The erosion effect resulting from particles with velocities less than the critical one is neglected.
- The effect of the tangential velocity component on particle deposition is neglected as the spray angle decreases from normal.

For powders used in thermal spray, the distribution of particle size can be expressed by the Rosin-Rammler formula (Ref 15):

$$f_m = \left\{ 1 - \exp \left[- \left(\frac{d_p}{d_0} \right)^m \right] \right\} \cdot 100\% \quad (\text{Eq 1})$$

where d_p is the particle diameter, f_m is the cumulative mass fraction of all particles with a diameter less than d_p , and d_0 and m are constants that are dependent on the powders used and can be determined experimentally.

In this model, by truncating the size range, Eq 1 can be modified as follows:

$$f_m = \left\{ 1 - \exp \left[- \left(\frac{d_p - d_{min}}{d_0} \right)^m \right] \right\} \cdot \left\{ 1 - \exp \left[- \left(\frac{d_{max} - d_{min}}{d_0} \right)^m \right] \right\}^{-1} \cdot 100\% \quad (\text{Eq 2})$$

where d_{max} and d_{min} are the maximum and minimum cutoff diameters of the particles. Therefore, the size of all particles ranges from d_{min} to d_{max} .

Besides particle size, particle velocity also depends on the nozzle expansion ratio and downstream length, particle density and shape factor, and parameters of driving gas including the type of the gas, its pressure, and temperature in cold spraying (Ref 10). Particle velocity, which is obtained by the simulation of a converging/diverging conically shaped spray nozzle, can be expressed by a simple empirical function (Ref 10). Consequently, the relation between particle velocity and individual parameters, such as particle diameter, can be obtained. In this case, according to the simulation result, particle velocity (V_p) at a certain standoff distance can be expressed empirically as follows, as the maximum particle velocity is lower than the gas stream velocity:

$$V_p = \frac{k}{d_p^n} \quad (\text{Eq 3})$$

where k and n are coefficients related to spray conditions for a certain material.

When the size of spray powder particles ranges from d_{min} to d_{max} , the particles of diameters d_{min} and d_{max} will achieve the maximum velocity (V_{max}) and the minimum velocity (V_{min}), respectively, in Eq 3. When V_{min} is higher than the critical velocity (V_c), all particles will be deposited on the coating surface, resulting in 100% deposition efficiency. On the other hand, when V_{max} is lower than V_c , no particle will be deposited, and the deposition efficiency is 0%. When V_c ranges from V_{min} to V_{max} , the maximum size of the particles (d_c) adhered to the substrate can be calculated from Eq 3 as follows:

$$d_c = \left(\frac{k}{V_c} \right)^{1/n} \quad (\text{Eq 4})$$

Thus, the deposition efficiency (E_d) can be obtained as a function of particle size by substituting Eq 4 into Eq 2 as follows:

$$E_d = \left\{ 1 - \exp \left[- \left(\frac{(k/V_c)^{1/n} - d_{min}}{d_0} \right)^m \right] \right\} \cdot \left\{ 1 - \exp \left[- \left(\frac{d_{max} - d_{min}}{d_0} \right)^m \right] \right\}^{-1} \cdot 100\% \quad (\text{Eq 5})$$

As the spray angle (θ) decreases from the normal angle (see Fig. 1), the normal component of particle velocity (V_n) can be described as follows:

$$V_n = \frac{k}{d_p^n} \cdot \sin(\theta) \quad (\text{Eq 6})$$

Therefore, d_c in the off-normal angle becomes:

$$d_c = \left(\frac{k \cdot \sin(\theta)}{V_c} \right)^{1/n} \quad (\text{Eq 7})$$

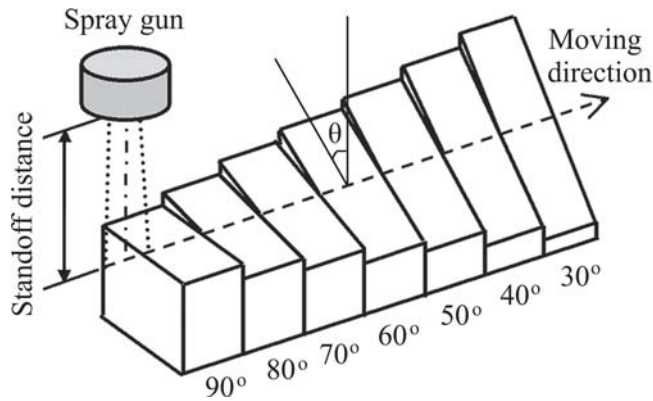


Fig. 1 Schematic diagram of the substrate fixture for spraying at different angles

The deposition efficiency at a given spray angle can be calculated by substituting Eq 7 into Eq 2:

$$E_d = \left\{ 1 - \exp \left[- \left(\frac{(k \cdot \sin(\theta) / V_c)^{1/n} - d_{min}}{d_0} \right)^m \right] \right\} \cdot \left\{ 1 - \exp \left[- \left(\frac{d_{max} - d_{min}}{d_0} \right)^m \right] \right\}^{-1} \cdot 100\% \quad (\text{Eq 8})$$

As the deposition efficiency at a given off-normal angle is normalized with that of a normal angle, the relative deposition efficiency (E_r) can be obtained as follows:

$$E_r = \left\{ 1 - \exp \left[- \left(\frac{(k \cdot \sin(\theta) / V_c)^{1/n} - d_{min}}{d_0} \right)^m \right] \right\} \cdot \left\{ 1 - \exp \left[- \left(\frac{(k / V_c)^{1/n} - d_{min}}{d_0} \right)^m \right] \right\}^{-1} \cdot 100\% \quad (\text{Eq 9})$$

Assuming that the minimum particle velocity is less than the critical velocity, the relative deposition efficiency against the spray angle is given by Eq 9. Because the constants concerning particle size distribution in Eq 2 and velocity distribution in Eq 3 can be known before the test, only the critical velocity is a function of the variables of relative deposition efficiency and spray angle. Therefore, if the relation between relative deposition efficiency and spray angle can be determined experimentally, the critical velocity can be calculated by best-fitting experimental data using Eq 9.

3. Numerical Simulation Method for Particle Velocity, Particle Temperature, and Adiabatic Shear Deformation on Impact

3.1 Particle Accelerating and Heating

The velocity and temperature of particles prior to impact on a substrate are calculated using a computational fluid dynamics

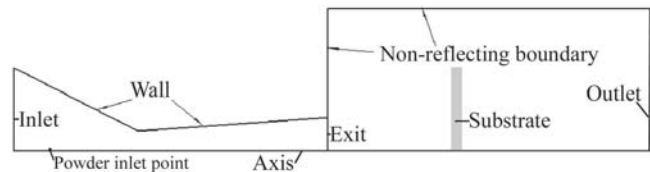


Fig. 2 Schematic diagram of the computational domain and boundaries for gas flow and particle acceleration

program, FLUENT (Fluent Inc., NH) (Ref 15). Owing to the axisymmetric characteristics of the flow in this study, a two-dimensional (2D) model is used. The schematic diagram of the computational domain and boundaries is shown in Fig. 2. For the determination of gas flow beyond the nozzle exit, the domain is extended to a cylindrical area with a radius of 60 mm and a length of 200 mm outside the nozzle exit. Meshing was conducted with the quadrangular element.

The accelerating gas is taken as an ideal, compressible gas. A coupled implicit method that is available from commercial software, FLUENT, is used to solve the flow field, and the flow field in a steady state is obtained. A second-order discretization scheme is used. The standard K- ϵ turbulence model is used. The accelerating and heating of particles are computed using discrete phase modeling, which is available from the FLUENT software. The effect of particle feeding on the gas flow field was not considered in this study. Regarding the heating of particles during gas stream, the temperature difference within a particle during heating was neglected, and the particle was therefore treated as isothermal. Other details on the simulation can be found in Ref 10 and 16.

In this simulation, spherical Cu particles with different diameters were used. The initial velocity and temperature of particles are 50 m/s and 27 °C, respectively. Gas conditions were set to those used in the experiment. The standoff distance of the substrate from the nozzle exit was 20 mm in the simulation.

3.2 Particle Impacting

The impacting behavior of the Cu particle on the Cu substrate is modeled using an explicit finite element analysis (FEA) program LS-DYNA (Livermore Software Technology Co., CA) (Ref 17). A Lagrangian formulation is used for the solution. Because the inertial force is the controlling factor during high-velocity impact processes, other forces, such as gravity, are neglected. The contact process is implemented by using an automatic, 2D, single-surface penalty formulation, which is available in LS-DYNA. By taking the thermal effect into account, a coupled structural/thermal analysis is performed. In addition, the thermal process is taken as adiabatic shear, and the heat conduction within particle is neglected. The temperature increase is based on the empirical assumption that 90% of the work from plastic deformation under adiabatic conditions is dissipated as heat (Ref 18).

Due to the axisymmetric characteristic of a normal impact process, a two-dimensional (2D) model is used, as shown in Fig. 3(a). The substrate is taken as a cylinder. According to the primary study, the radius and height of the substrate are taken as 10 times the particle diameter (20 μm) to avoid the effect of calculating dimensions on the accuracy of the deformation zone.

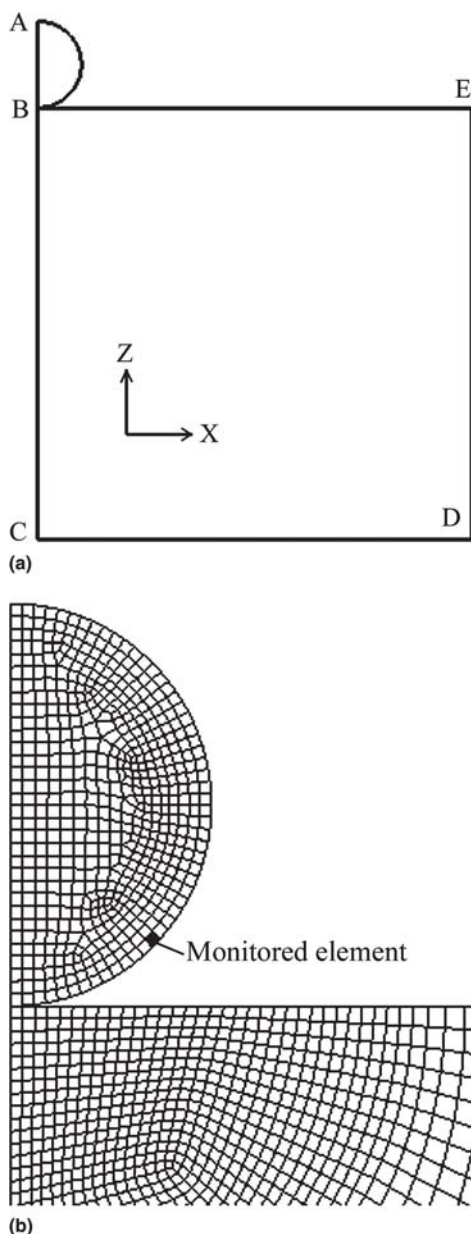


Fig. 3 (a) Geometric model of particle impact and (b) the meshing of the particle and the local contact zone in the substrate

Meshing is conducted by using a four-node 2D quad element with 1-point integration, as shown in Fig. 3(b). The meshing size for particles is $0.625 \mu\text{m}$ except the case of a specific statement indicating the meshing size used. Moreover, the local contact zone in the substrate, which also experiences intensive deformation, is meshed with fine meshing to ensure accuracy, as shown in Fig. 3(b). The monitored element that is used for output is also marked in Fig. 3(b). In the simulations, the boundary A-B-C, as shown in Fig. 3(a), is constrained in X displacement, and the boundary C-D is constrained in Z displacement. Other boundaries are free to move.

As for the material model, the Cu particle and substrate are taken as a Johnson and Cook plasticity model, which accounts for strain hardening, strain rate hardening, and thermal soften-

Table 1 Properties of Cu used in this study (Ref 18)

Property	Value
Density, kg/m^3	8960
Heat capacity, $\text{J}/(\text{kg} \cdot \text{K})$	383
Thermal conductivity, $\text{W}/(\text{m} \cdot \text{K})$	386
Young's modulus, GPa	124
Poisson's ratio	0.34
A , MPa	90
B , MPa	292
N	0.31
C	0.025
M	1.09
T_m , K	1356
T_{room} , K	298
Reference strain rate, 1/s	1

ing. The Von Mises plasticity model is used. The yield stress (σ_y) of this material is expressed as follows (Ref 17, 18):

$$\sigma_y = (A + B\varepsilon_{eff}^p)^N (1 + C \ln \varepsilon^*) (1 - T^{*M}) \quad (\text{Eq 10})$$

where A , B , N , C , and M are user-defined input constants, ε_{eff}^p is the effective plastic strain, ε^* is the effective plastic strain rate normalized with respect to a reference strain rate, and T^* is a homologous temperature that is defined as follows (Ref 17, 18):

$$T^* = \frac{T - T_{room}}{T_m - T_{room}} \quad (\text{Eq 11})$$

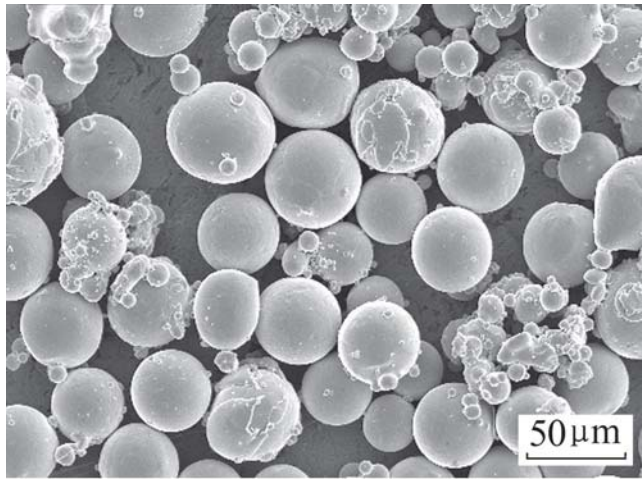
where T_m is the melting point and T_{room} is the reference temperature. A linear Mie-Gruneisen equation of state is used (Ref 17).

An isotropic thermal material is used. The properties of the Cu used in the simulation are shown in Table 1 (Ref 18).

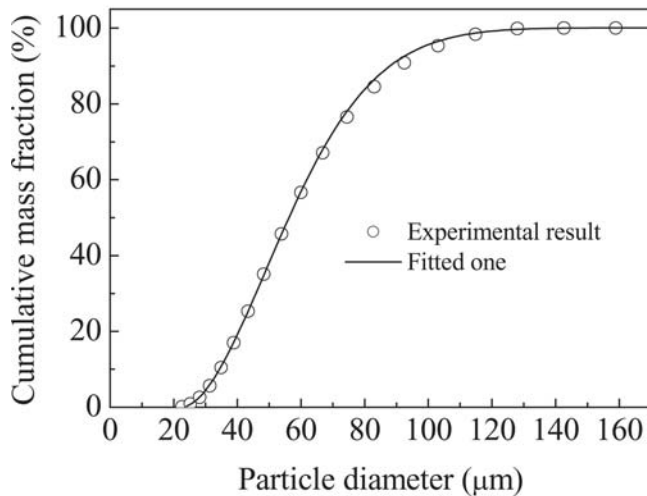
4. Materials and Experimental Procedures

A commercially available Cu powder with an average particle size of $56 \mu\text{m}$ was used as feedstock (denoted as the powder P-A in this study). The oxygen content of this powder was determined to be $\sim 0.01 \text{ wt.}\%$ using an oxygen determinator (RO-316; LECO, MI). The powder was produced by a gas atomization process and exhibited spherical morphology, as shown in Fig. 4(a). To obtain a reliable relationship between the deposition efficiency and the spray angle, the size distribution of Cu powder was characterized by a laser diffraction sizer (MASTERSIZER 2000; Malvern Instruments Ltd., Malvern, U.K.). The size distribution was fitted using the modified Rosin-Rammler formula to obtain a relation between the cumulative mass fraction and particle diameter. A comparison of the fitted relation with experimental observation is shown in Fig. 4(b). It is shown that the size distribution of Cu powder used in this study is well represented by the modified Rosin-Rammler formula. The fitting yielded the constants $41.2 \mu\text{m}$ for d_0 , 1.8 for m , $142.6 \mu\text{m}$ for d_{max} , and $22.6 \mu\text{m}$ for d_{min} . The Cu plate that was used as a substrate had dimensions of $45 \times 15 \times 3 \text{ mm}$. It was grit-blasted with 24-mesh alumina grits prior to spray.

A cold-spraying system that was developed at Xi'an Jiaotong University was used to produce the coating. The design of the



(a)



(b)

Fig. 4 (a) Morphology of Cu powder (type P-A) used and (b) its size distribution obtained experimentally and fitted by a modified Rosin-Rammler formula

Table 2 Constants k and n , and mean particle temperature for different gas conditions in this study for powder P-A

Condi- tion	Gas	Pressure, MPa	Tempera- ture, °C			Mean particle temperature, °C
				k	n	
C1	N ₂	2.0	265	1231.3	0.36	41
C2	N ₂	2.0	400	1299.0	0.36	82
C3	N ₂	2.0	540	1347.5	0.36	122
C4	He	1.0	165	1530.3	0.36	-80

system has been described in detail elsewhere (Ref 11). A converging-diverging de Laval nozzle with a conical shape was adopted. The throat diameter is 2 mm. The expansion ratio of the nozzle was 9, and the downstream length from the throat to the exit was 100 mm. Nitrogen and helium were used as accelerating gases under different conditions, as shown in Table 2. The powder carrier gas is the same as the main gas. The substrate was

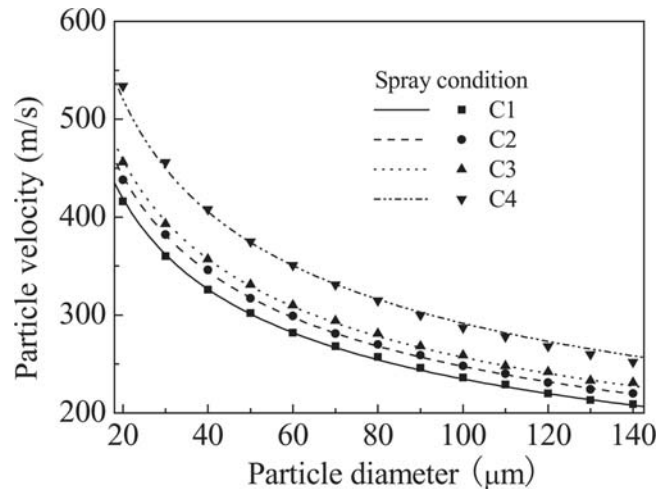


Fig. 5 Change of particle velocity with particle diameter under different gas conditions for powder P-A. The points are data obtained by numerical simulation, and lines are those calculated by the fitted equation.

fixed at a specially designed fixture, as shown in Fig. 1. The standoff distance was 20 mm from the nozzle exit to the center of the substrate surface. During deposition, the spray gun was manipulated by a robot and traversed at a speed of 80 mm/s across the substrate. All specimens at different angles were prepared in one pass. The weight gain of each specimen after deposition was measured using a balance with a precision of 0.1 mg. Specimen weighing was carried out for each spray condition. The relative deposition efficiency was evaluated by the ratio of the weight gains of the specimens placed at different tilting angles to that of the specimen sprayed at the normal angle.

5. Results

5.1 Particle Velocity and Temperature

Under the spray conditions shown in Table 2, the constants k and n in Eq 3 are obtained through numerical simulation. Figure 5 shows the effect of particle size on particle velocity under different gas conditions calculated using the parameters shown in Table 2. Those results clearly show that particle velocity decreases with the increase in particle diameter. Moreover, particle velocity increases with an increase in gas temperature. When using helium as the driving gas, the particles can be accelerated to a higher velocity than that using nitrogen under all three conditions cited in Table 2.

On the other hand, the calculated mean particle temperature corresponding to a particle size of 56 μm increases with nitrogen temperature, as shown in Table 2. While using helium, the mean particle temperature is much lower than that of nitrogen.

5.2 Adiabatic Shear Instability of Particle Deformation

Figure 6 shows the effect of particle velocity and temperature on the compression ratio of the particle. The compression ratio (R_c) of the particle is defined as:

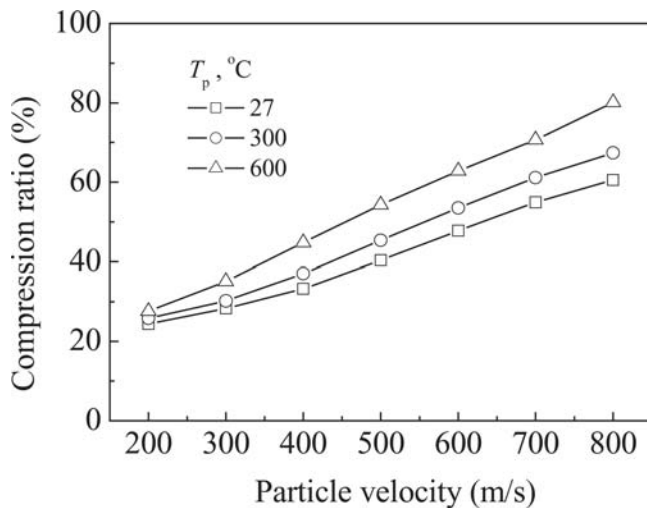


Fig. 6 Effect of particle velocity on its compression ratio under different particle temperatures

$$R_c = \frac{d_p - h_p}{d_p} \cdot 100\% \quad (\text{Eq 12})$$

where h_p is the height of the deformed particle. It is clear that with the increase in particle velocity the compression ratio increases almost linearly. That means that the particle deforms more intensively with the increase in particle velocity. Moreover, with the increase in particle temperature the compression ratio also increases evidently, especially at a high particle velocity. This is because the thermal softening effect occurs at elevated temperatures.

At the localized contact interface, particles deform more intensively. Figure 7 shows the simulated temporal development of the effective plastic strain of the monitored element under different particle velocities. It is found that as the impact process progresses the effective plastic strain increases. It is observed that when the particle velocity is higher than 410 m/s, the effective plastic strain increases rapidly at a certain impact time. This means that the adiabatic shear instability occurs as the particle velocity is higher than 410 m/s. Assadi et al. (Ref 13) has pointed out that the velocity for the onset of adiabatic shear instability corresponds to the critical velocity for particle deposition. However, it was also found in this study that the meshing size in simulation has a significant influence on the critical particle velocity to cause the shear instability at the localized contact area. Although the numerical critical velocity calculated by Assadi et al. (Ref 13) agreed with their experimental result, the effect of mesh size on the simulation results should be further clarified.

Figure 8 shows the effect of meshing size on the critical velocity causing the shear instability of Cu particles under different temperatures. It is clear that with the decrease in mesh size the velocity for the onset of shear instability decreases significantly for the temperature of each particle. Furthermore, with the increase in particle temperature the critical velocity decreases. In FEA, the smaller the mesh size, the more accurate the result. Therefore, a mesh size of zero will yield the critical velocity. The extrapolation of the critical velocity to a mesh size of zero would approach a reasonable critical velocity for particle deposition.

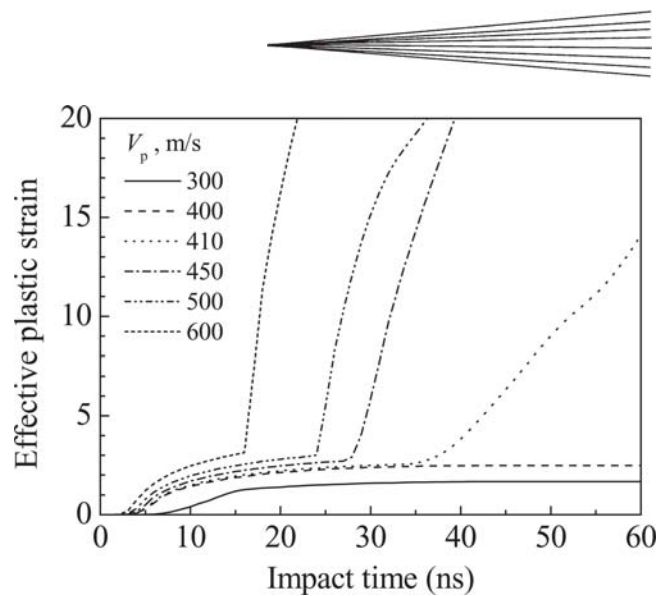


Fig. 7 Simulated temporal development of the effective plastic strain of the monitored element under different particle velocities

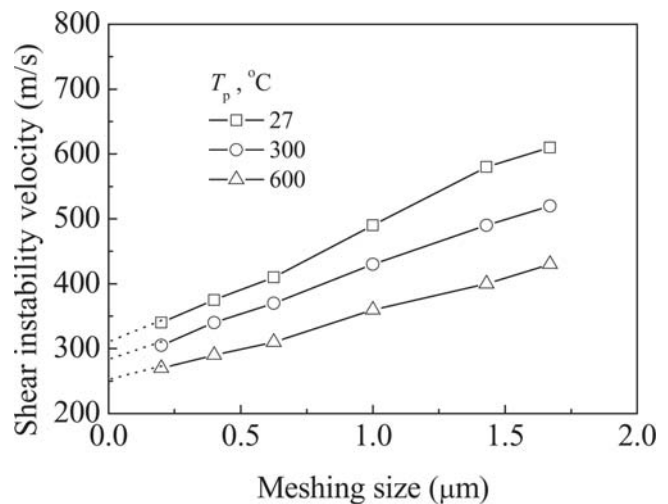


Fig. 8 Effect of meshing size on the shear instability velocity of a Cu particle under different temperatures. Extrapolation of the shear instability velocity to zero meshing size yields velocities of approximately 310, 290, and 250 m/s at particle temperatures of 27, 300, and 600 °C, respectively.

Consequently, the extrapolation of shear instability velocity to a zero meshing size yielded critical velocities of approximately 310, 290, and 250 m/s at particle temperatures of 27, 300, and 600 °C, respectively. Although those values are much lower than those previously reported in the literature (Ref 1, 5, 7), they agree well with the experimental results. It is considered that the underlying reason for this large discrepancy between the reported critical velocities (Ref 1, 5, 7) and the results obtained above is the oxygen content of the feedstock, which is discussed in the next section of this article.

5.3 Effect of Particle Condition on the Critical Velocity

Figure 9 shows the effect of an off-normal spray angle on the relative deposition efficiency of Cu particles under four different

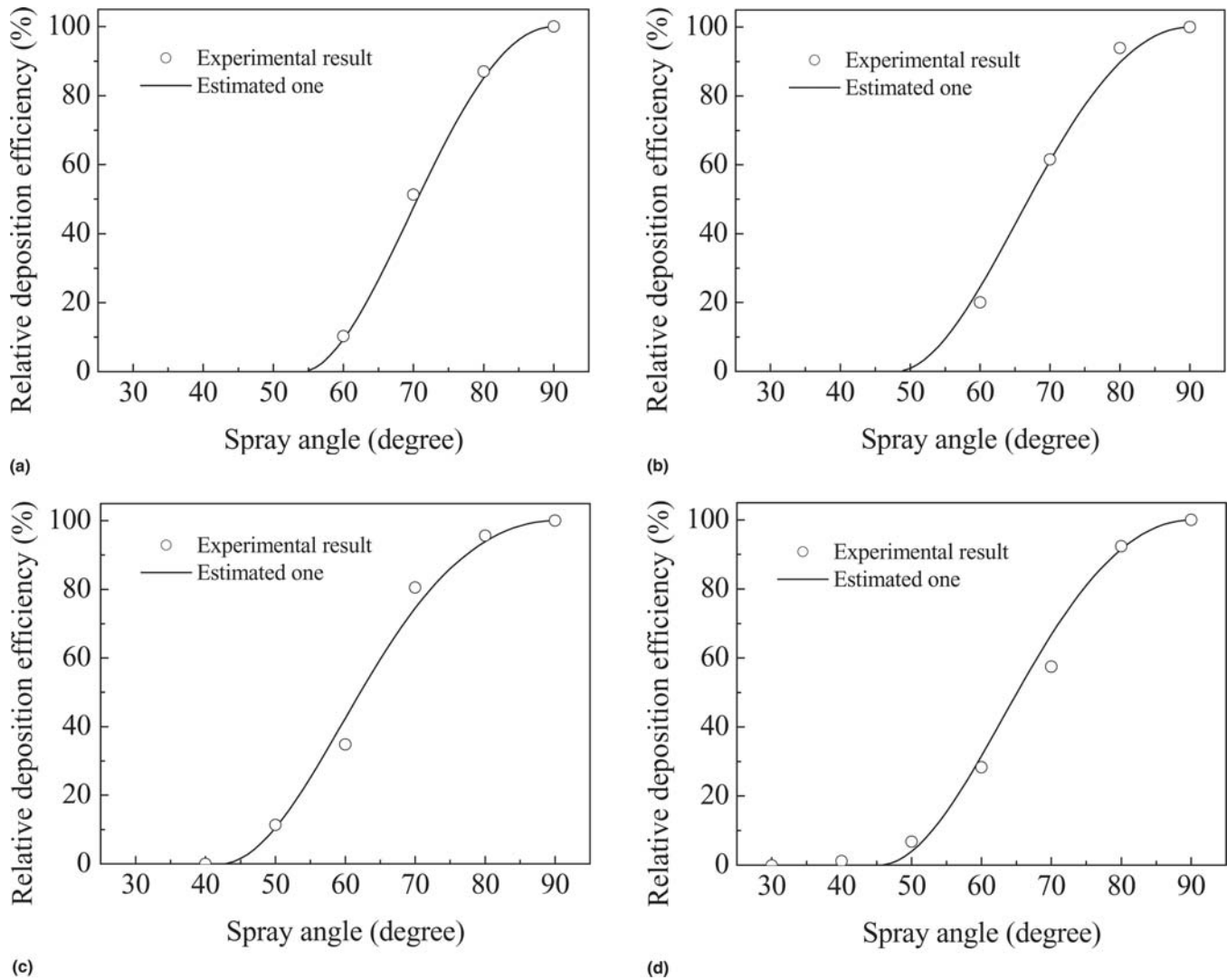


Fig. 9 Comparison of the relative deposition efficiency versus the spray angle calculated theoretically with those observed under gas conditions (a) C1, (b) C2, (c) C3, and (d) C4

particle conditions. Clearly, with the decrease in spray angle from normal the relative deposition efficiency decreases under the four gas conditions. There exists a critical spray angle for each condition, below which no particles are successfully deposited. The critical spray angle also changed with particle condition. By least squares fitting of the relative deposition efficiency with the spray angle using Eq 9, the critical velocity of particle deposition can be obtained. The solid lines in Fig. 9 represent the calculated results using fitted equations. It demonstrates that the fitted results depicted the observed relation between the relative deposition efficiency and the spray angle well.

The critical velocities obtained through such a fitting approach are 327, 318, 298, and 356 m/s, respectively, for gas conditions C1, C2, C3, and C4. Therefore, the critical particle velocity changes with the spray particle conditions.

As predicted by numerical simulation, the mean particle temperatures under conditions C1, C2, C3, and C4 were much different, as shown in Table 2. It is suggested that the change in the critical velocity is attributed to the change in particle tempera-

ture. Figure 10 shows the effect of particle temperature on the critical velocity. Evidently, with the increase in particle temperature the critical velocity decreases significantly. This change can be attributed to a thermal softening effect. For comparison, the critical velocities for the occurrence of adiabatic unstable flow that were obtained through numerical simulation under different particle temperatures (i.e., calculated critical velocity) are also shown in Fig. 10. It is clear that the observed results agreed reasonably with the calculation. This fact suggests that the critical velocity obtained through the relationship between relative deposition efficiency and spray angle is reasonable. However, it was observed that a deviation of the calculated data one from the experimental data becomes large when the particle temperature decreases to room temperature. This fact may be due to the uncertainty of the materials model used in the current study. The results clearly show that the critical velocity of particle deposition decreases with an increase in particle temperature. Following those results, the critical velocity will decrease by about 14 m/s with a temperature increment of 100 °C.

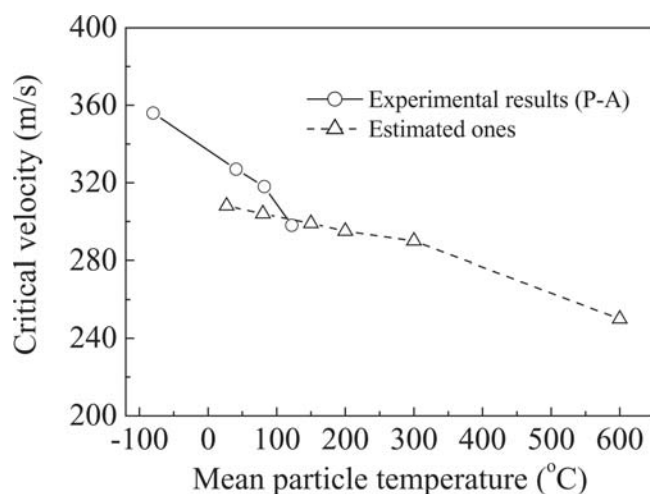


Fig. 10 Effect of mean particle temperature on critical velocity comparing the numerical simulation result with the measured result

6. Discussion

6.1 Feasibility of the Measurement Approach for the Critical Velocity in Cold Spraying

6.1.1 Effect of Particle Size Distribution Based on the theoretical relationship between the relative deposition efficiency and spray angle established using a modified Rosin-Rammler formula, it is possible to estimate the critical velocity in cold spraying. The experimental test confirmed that the test data correlated well with the theoretical relation. It was also clear that the critical velocity of particles of a size distribution can be measured by the approach proposed above.

In deriving the theoretical Eq 9, it was suggested that the critical velocity is independent of particle size. To clarify the effect of powder particle size distribution on the test result for critical velocity, a powder (referred to as powder P-B) that was sieved out from commercial spherical Cu powder was used. This powder had a mean particle size that was about half that of powder P-A. The particle size distribution of this powder is shown in Fig. 11. It was also found that the modified Rosin-Rammler formula in this study described the powder size distribution well. The constants for the Rosin-Rammler formula for this powder were 26 μm , 1.9 μm , 60.1 μm , and 2.2 μm , respectively, for d_0 , d_{\min} , d_{\max} , and m . A deposition test using this powder was carried out using N_2 at a pressure of 2.0 MPa and a temperature of 490 °C. Figure 12 shows the results of the test of the relationship between the relative spray deposition efficiency and the spray angle in comparison with the fitted relation. With this test, due to high deposition efficiency, the relative deposition efficiency at a spray angle of 80° is almost equal to that at 90°. Consequently, the correlation was performed with the data for an 80° spray angle as a reference rather than those for the 90° spray angle. In this case, the relative deposition efficiency is taken as 100%. The fitting yielded a critical velocity of 310 m/s.

From the gas temperatures, it was estimated that the mean particle temperature for powder P-B prior to impact was about 80 °C higher than that of powder P-A under condition C2 in this study. According to the finding in the previous section, increas-

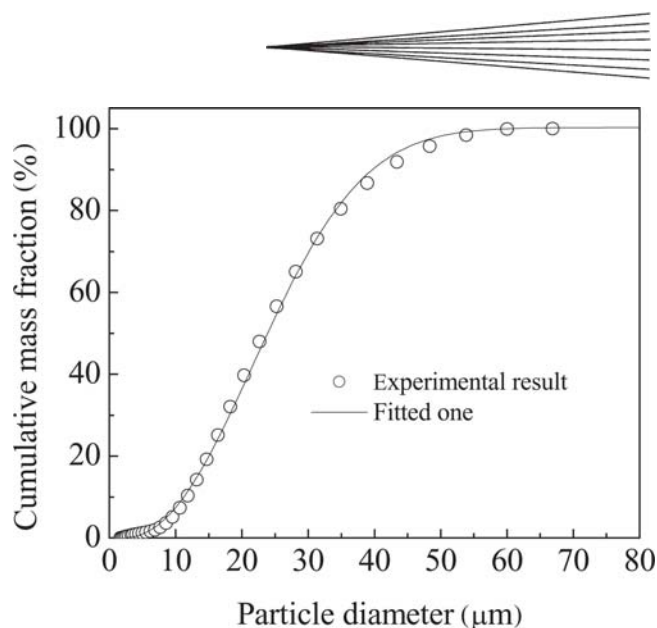


Fig. 11 Comparison of the size distribution of Cu powder (type P-B) between the measured size and the fitted size determined by the Rosin-Rammler formula

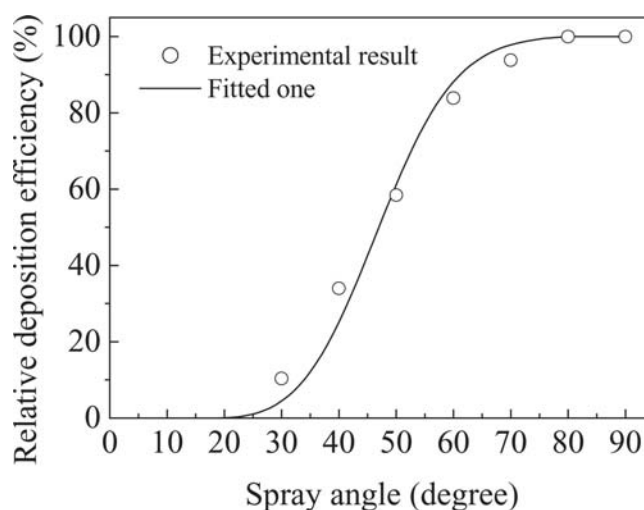


Fig. 12 Relative deposition efficiency versus spray angle for powder P-B comparing the measured data with the fitted result using the proposed equation in the current study

ing particle temperature will reduce the critical velocity at a rate of 14 m/s per 100 °C increment for Cu particles. Therefore, the critical velocity of a P-B Cu particle at the same temperature as that under condition C2 should be about 11 m/s higher. This yielded a critical velocity of 321 m/s, which is almost the same as the 318 m/s for the P-A powder under condition C2. This result provided evidence that critical velocity is independent of particle size. Moreover, this fact suggests that the change in the critical velocity can be detected by the present method.

6.1.2 Effect of Particle Velocity Distribution The experiments were carried out to clarify the effect of particle velocity distribution on critical velocity. Two velocity distributions that were different from those obtained under spray condition C2 in Table 2 were created using type P-A powder through changing

the accelerating gas pressures from 1.0 to 2.6 MPa, as shown in Table 3. The gas temperature was maintained at ~ 400 °C during spraying for those two conditions.

The average particle velocities for those two conditions were 260 and 325 m/s, respectively, for particles of the same mean diameter. The constants are shown in Table 3. The relations fitted using Eq 9 were also shown in Fig. 13 for two conditions. The best fitting yielded critical velocities of 316 and 319 m/s, respectively, for two particle velocity distributions corresponding to spray conditions C5 and C6. Taking account of the critical velocity of 318 m/s that was obtained under particle condition C2, it is clear that the measured critical velocity is independent of the particle velocity distribution. Those results are reasonable because the critical velocity should be independent of the particle velocity distribution. Moreover, these results clearly showed that for certain particles under a comparable gas temperature the critical velocity is well defined.

In the test described above, the particle temperature on impact is considered to be the same for all particles of different sizes. The calculation of the effect of particle size on temperature showed that temperature is only significantly influenced by particle size as particle size becomes <20 μm (Ref 19). No significant temperature change was found as particle size increased to >20 μm . On the other hand, as particle size changed from 5 to 20 μm , the change in particle temperature was limited to about 100 °C. This temperature difference will cause a test error on a critical velocity ~ 10 m/s, as discussed above. Therefore, a test using a large particle size may decrease the test error.

6.1.3 Effect of Oxygen Content Copper has been used as a typical material for cold spraying by many investigators. Accordingly, the critical velocity of copper particles has been reported by several investigators. For example, critical velocities of 500 m/s (Ref 1), 550 to 570 m/s (Ref 5), and 640 m/s (Ref 7) can be found in different reports. It can be noticed that those results are much higher than the results obtained in this report. A comparison of the compositions of the starting materials used showed a clear difference in the oxygen content of Cu powders used by different investigators. Compared with the oxygen content of 0.01 wt.% in Cu powder P-A and 0.02 wt.% in Cu powder P-B used in this study, the oxygen content of Cu powders used by other investigators varied from 0.1 wt.% (Ref 5) to 0.336 wt.% (Ref 7). To ascertain the feasibility of the present approach, a test was performed using two Cu powders of higher oxygen content (i.e., 0.14 and 0.38 wt.%). The particle sizes of these two powders were similar to that of powder P-B, but they were oxidized in a furnace under ambient conditions. After oxidation, the oxygen content was increased by an order of magnitude compared with the original one. Figures 14(a) and (b) show the test results for relative deposition efficiency versus spray angle that were obtained using oxidized powders with oxygen contents of 0.14 and 0.38 wt.%, respectively. From these results, critical velocities of 550 and 610 m/s, respectively, were obtained. Stoltenhoff et al. (Ref 5) reported a critical velocity of 570 m/s for a Cu powder with an oxygen content of 0.1 wt.%. In their recent article, Gärtner et al. (Ref 20) reported a critical velocity of 550 m/s for similar Cu powders with an oxygen content of ~ 0.2 wt.%. Gilmore et al. (Ref 7) reported a critical velocity of 640 m/s for a Cu powder with an oxygen content of 0.336 wt.%. Taking account of the measurement error pointed out by Gärtner et al. (Ref 20), it can clearly be recognized that the results of the

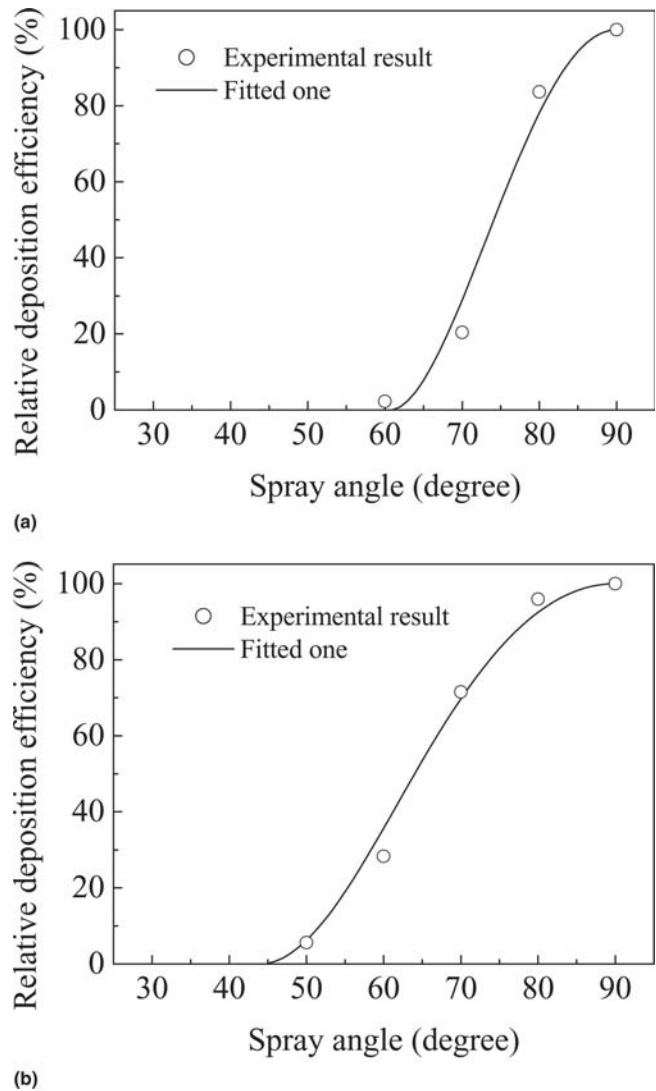
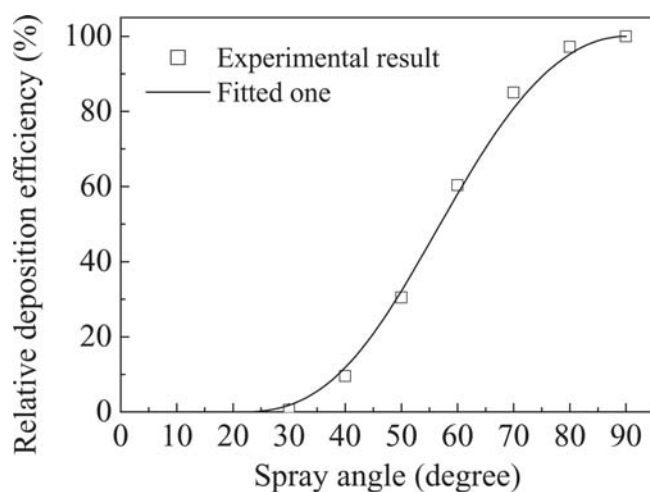


Fig. 13 Relative deposition efficiency versus spray angle at different particle velocity distributions obtained under different conditions comparing the measured data with the fitted result. (a) condition C5; (b) condition C6

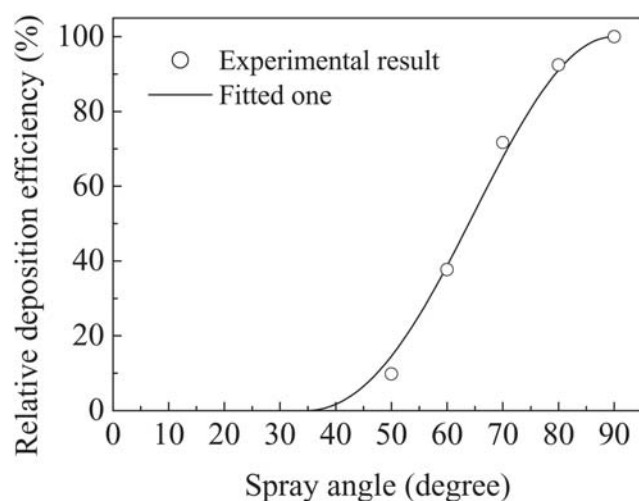
Table 3 Constants k and n for powder P-A for the study of the effect of particle velocity distribution

Condition	Gas	Pressure, MPa	Temperature, °C	k	n
C5	N ₂	1.0	400	1231.3	0.36
C6	N ₂	2.6	400	1347.5	0.36

current study, which were obtained by oxidizing Cu powders to different oxygen content levels, are reasonably consistent with those reported previously. Therefore, it is clear that the present approach can also detect a change in the critical velocity that is due to a variation in particle conditions. On the other hand, it has been clearly revealed that the oxidization condition of the spray powder has a significant impact on the critical velocity and coating bond strength in cold spraying, as has been discussed in detail elsewhere (Ref 21).



(a)



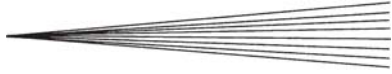
(b)

Fig. 14 The relationship between the relative deposition efficiency and the spray angle measured for the oxidized Cu powders compared with the fitted results. Oxygen content of Cu powders: (a) 0.14 wt.%; (b) 0.38 wt.%

As a result, the large discrepancy among the critical velocities for Cu particles obtained by different investigators is attributed to the difference in the oxide content of the powder. A high oxygen content results in a high critical velocity.

6.2 Questions on Estimation of the Critical Velocity Through Numerical Simulation

The recent investigation of solid metal particle impact on a metal substrate suggests that critical velocity in cold spraying can be estimated through the numerical simulation of particle deformation behavior on impact (Ref 13). The study also confirmed this possibility. This fact was also further confirmed by Grujicic et al. (Ref 22). However, it is clear that the simulated critical velocity of about 300 m/s that was obtained in our study for a Cu particle impacting on a Cu substrate is much different from those of about 580 m/s, as previously reported (Ref 13). As revealed by the results in this study, the critical velocity esti-



mated through numerical simulation will be significantly influenced by the detailed simulation conditions. For example, it was demonstrated that the simulated critical velocity is influenced by meshing size. But, based on the result obtained in the study, this influence should be limited by taking into account the difference in the critical velocity reported from this study from those critical velocities reported in the literature (Ref 13, 22). According to the experimental test results in this study, it can be believed that the simulation results in this study are reasonable and convincing, because the results derived from simulation and experimentation are consistent. By comparing the conditions used in the authors simulation study with those reported in the literature (Ref 13, 22), it can be found that both material models and constants were the same in all simulation studies, including the current study except in the use of different software. It could be considered that the high oxygen content of the Cu powder that resulted in a high critical velocity in the experiment by Assadi et al. (Ref 13) was coincidentally consistent with the simulation result, which covered the problem discussed above. Therefore, it is still an open question as to what factors contributed to the significantly different results of the simulation study and how to obtain a convincing critical velocity for particle deposition through numerical simulation.

7. Conclusions

The critical velocity for particle deposition in cold spraying was investigated through numerical simulation and experiment using Cu powders. An experimental measurement method for determining the critical velocity was proposed based on the measurement of the relative deposition efficiency at different spray angles. With the present measurement method, the critical velocity can be determined only by measuring relative deposition efficiencies at different spray angles combined with the particle velocity distribution, which can be easily obtained using commercial software. The test results proved the feasibility of the proposed method to measure critical velocity in cold spraying without measuring particle velocity but using the particle velocity distribution obtained by numerical simulation using commercially available software.

It was confirmed that the critical velocity measured is independent of the particle size distribution and particle velocity distribution. The critical velocity depends on the particle temperature and is affected by its oxidizing condition. The critical velocity obtained, which depends on particle temperature, ranged from 298 to 356 m/s for pure Cu. The critical velocity decreased with an increase in particle temperature.

The current study shows a significantly lower critical velocity when Cu powder with a low oxide content is used. Experiments using Cu powders with higher oxide contents yielded comparable results to those reported in the literature. It was shown that the large discrepancy between the critical velocity obtained in this study and those reported previously can be attributed to the oxide content of the powder. A high oxygen content in the powder results in a higher critical velocity for particle deposition.

The critical velocity estimated through the numerical simulation of particle impact that induced an unstable flow agreed well with that derived from experimental observation. More-

over, the good agreement between the measured and the calculated critical velocities supports the rationale of the simulation method for the certain degree of accuracy used in this study. However, to use the numerical simulation method to estimate the critical velocity, it is still necessary to clarify what contributed to the large difference in critical velocity between that obtained in this study and those obtained in other previous studies.

Acknowledgments

This work was supported by the National Natural Science Foundation of China (grant No. 50171052) and by the Doctoral Foundation of Xi'an Jiaotong University.

References

1. A.P. Alkimov, V.F. Kosarev, and A.N. Papyrin, A Method of Cold Gas Dynamic Deposition, *Dokl. Akad. Nauk SSSR*, 1990, **318**(5), p 1062-1065
2. R.S. Lima, J. Karthikeyan, C.M. Kay, J. Lindemann, and C.C. Berndt, Microstructural Characteristics of Cold-Sprayed Nanostructured WC-Co Coatings, *Thin Solid Films*, 2002, **416**(1-2), p 129-135
3. C.-J. Li, G.-J. Yang, X.-C. Huang, W.-Y. Li, and A. Ohmori, Formation of TiO₂ Photocatalyst Through Cold Spraying, *Thermal Spray 2004: Advances in Technology and Application*, ASM International, May 10-12, 2004 (Osaka, Japan), ASM International, 2004, p 345-349.
4. T.H. Van Steenkiste, J.R. Smith, R.E. Teets, J.J. Moleski, D.W. Gorkiewicz, R.P. Tison, D.R. Marantz, K.A. Kowalsky, W.L. Riggs, P.H. Zajchowski, B. Pilsner, R.C. McCune, and K.J. Barnett, Kinetic Spray Coatings, *Surf. Coat. Technol.*, 1999, **111**(1), p 62-71
5. T. Stoltenhoff, J. Voyer, and H. Kreye, Cold Spraying: State of the Art and Applicability, *International Thermal Spray Conference*, E. Lugscheider and C.C. Berndt, Ed., March 4-6, 2002 (Essen, Germany), DVS Deutscher Verband für Schweißen, 2002, p 366-374.
6. D. Zhang, P.H. Shipway, and D.G. McCartney, Particle-Substrate Interactions in Cold Gas Dynamic Spraying, *Thermal Spray 2003: Advancing the Science and Applying the Technology*, B.R. Marple and C. Moreau, Ed., May 5-8, 2003 (Orlando, FL), ASM International, 2003, Vol. 1, p 45-52
7. D.L. Gilmore, R.C. Dykhuizen, R.A. Neiser, T.J. Roemer, and M.F. Smith, Particle Velocity and Deposition Efficiency in the Cold Spray Process, *J. Thermal Spray Technol.*, 1999, **8**(4), p 576-582
8. R.C. Dykhuizen and M.F. Smith, Gas Dynamic Principles of Cold Spray, *J. Thermal Spray Technol.*, 1998, **7**(2), p 205-212
9. T.H. Van Steenkiste, J.R. Smith, and R.E. Teets, Aluminum Coatings via Kinetic Spray with Relatively Large Powder Particles, *Surf. Coat. Technol.*, 2002, **154**(2-3), p 237-252
10. C.-J. Li and W.-Y. Li, Optimization of Spray Conditions in Cold Spraying Based on the Numerical Analysis of Particle Velocity, *Trans. Non-ferrous Met. Soc. China*, **14**(Special 2), 2004, p 43-48
11. C.-J. Li and W.-Y. Li, Deposition Characteristics of Titanium Coating in Cold Spraying, *Surf. Coat. Technol.*, 2003, **167**(2-3), p 278-283
12. C.-J. Li, W.-Y. Li, Y.-Y. Wang, G.-J. Yang, and H. Fukunuma, A Theoretical Model for Prediction of Deposition Efficiency in Cold Spraying, *Thin Solid Films*, 2005, **485**, p 79-85
13. H. Assadi, F. Gärtner, T. Stoltenhoff, and H. Kreye, Bonding Mechanism in Cold Gas Spraying, *Acta Mater.*, 2003, **51**(15), p 4379-4394
14. W.-Y. Li, C.-J. Li, Y.-Y. Wang, and G.-J. Yang, Effect of Cu Particle Parameters on Its Impacting Behavior in Cold Spraying, *Acta Metall. Sin.*, 2005, **41**(3), p 282-286, in Chinese
15. Fluent Inc., NH, *FLUENT Manual*, 1999
16. C.-J. Li and W.-Y. Li, Optimal Design of a Novel Cold Spray Gun Nozzle at a Limited Space, *J. Thermal Spray Technol.*, 2005, **14**(3), p 391-396
17. Livermore Software Technology Corporation, CA, *LS-DYNA Theoretical Manual*, 1998
18. G.R. Johnson and W.H. Cook, Fracture Characteristics of Three Metals Subjected to Various Strains, Strain Rates, Temperatures and Pressures, *Eng. Fract. Mech.*, 1985, **21**(1), p 31-48
19. C.-J. Li, W.-Y. Li, and G.-J. Yang, Examination of Impact Fusion Phenomenon During Cold Spraying of Zinc, *Thermal Spray 2004: Advances in Technology and Application*, ASM International, May 10-12, 2004 (Osaka, Japan), ASM International, 2004, p 335-340
20. F. Gärtner, T. Stoltenhoff, T. Schmidt, and H. Kreye, The Cold Spray Process and Its Potential for Industrial Applications, *Thermal Spray Connects: Explore Its Surface Potential*, E. Lugscheider, Ed., May 2-4, 2005 (Basel, Switzerland), DVS, p 158-163
21. C.-J. Li, W.-Y. Li, and H.-L. Liao, "Significant Influence of Particle Surface Oxidation on the Critical Velocity for Particle Deposition, Interface Microstructure and Adhesive Strength of the Deposited Coatings in Cold Spraying," Thermal Spray Laboratory Report of Xi'an Jiaotong University, 2005
22. M. Grujicic, C.L. Zhao, W.S. DeRosset, and D. Helfritsch, Adiabatic Shear Instability Based Mechanism for Particle/Substrate Bonding in the Cold-Gas Dynamic-Spray Process, *Mater. Des.*, 2004, **25**(8), p 681-688